

Palladium nanocrystals and their properties

E. CZERWOSZ^{1*}, P. DŁUŻEWSKI², J. KĘCZKOWSKA³,
M. KOZŁOWSKI^{1,2}, M. SUCHAŃSKA³, H. WRONKA¹

¹ Tele&Radio Research Institute, ul. Długa 44/50, 00-241 Warsaw, Poland

² Institute of Physics PAN, al. Lotników 36/46, 02-668 Warsaw, Poland

³ Kielce University of Technology, al. 1000-lecia PP 7, 25-312 Kielce, Poland

Films composed of Pd nanocrystals embedded in fullerene C₆₀ matrix have been studied by TEM, AFM, UV-VIS absorption methods. Data on the structure of Pd nanocrystals was obtained from electron diffraction of selected areas and the size distribution for Pd nanocrystals was found from dark field TEM images. UV-VIS absorption spectra showed the shift of C₆₀ characteristic bands connected with the ligand field effect. Electric characteristics were recorded for the initial dry film and film wetted by various liquid agents (benzene, ethanol, toluene).

Key words: *palladium nanocrystals; TEM; AFM; UV-VIS absorption; electric properties*

1. Introduction

Grain boundaries make up a major portion of a material in the nanoscale, and strongly affect its properties and processing. Properties of nanomaterials deviate from those of single crystals or polycrystals and glasses with the same average chemical composition. This deviation results from the size and dimensionality of nanometer-sized crystallites as well as from numerous interfaces between crystallites. Nanocrystallites of bulk inorganic solids exhibit size dependent properties such as lower melting points, higher energy gaps, and nonthermodynamic structures [1, 2]. In comparison to macro-scale powders, increased ductility has been observed in nanopowders of metal alloys [2, 3].

One of the primary applications of metals such as Pd is their use as heterogeneous catalysts in a variety of reactions. Due to their vastly increased surface area over macro-scale, palladium and its compounds are ultra-high activity catalysts. They are also used as starting materials for a variety of reactions.

*Corresponding author, e-mail: czerwosz@pie.edu.pl

Palladium and its compounds show a high and selective affinity towards hydrogen, resulting in their volume expansion. Fibre Bragg gratings attached to palladium elements are used to monitor the resultant strain from the hydrogen uptake. The technique is aimed at monitoring hydrogen at low concentrations, down to a few hundred ppm, where H_2 is the result of polymer materials ageing [4]. All palladium sensors are based on the phenomena of adsorption and dissociation of hydrogen containing molecules.

In this paper, we show a new method of preparation of Pd nanocrystals embedded in fullerene matrix. The system exhibits properties predisposing it to apply it as a liquid sensing element.

2. Experimental

Pd nanocrystalline films were prepared by the physical vacuum deposition method (PVD) by evaporation from two separated sources of fullerene C_{60} and palladium acetate. The films were deposited on various substrates (glass, Si, metal foils). The distance from the sources to the substrate was the same for all processes. The composition and film structure changed upon changing temperatures of the sources.

The structures, morphologies, topographies and compositions of the films were studied by the transmission electron microscopy (TEM) with the electron diffraction of selected area method (EDSA), atomic force microscopy (AFM) and atomic absorption spectroscopy analysis (ASA). Electronic properties of fullerene based matrices were studied by absorption spectroscopy in the UV-VIS region. The changes in film resistivities were studied using the experimental set-up presented in Fig. 1. A sample was placed in a special holder (Fig. 1a). The holder was prepared in a special way allowing one to omit the problem of preparation of metallic electric contacts. The electric contacts in the holder were realized only by a mechanic contact of a metal tip with the surface of the film.

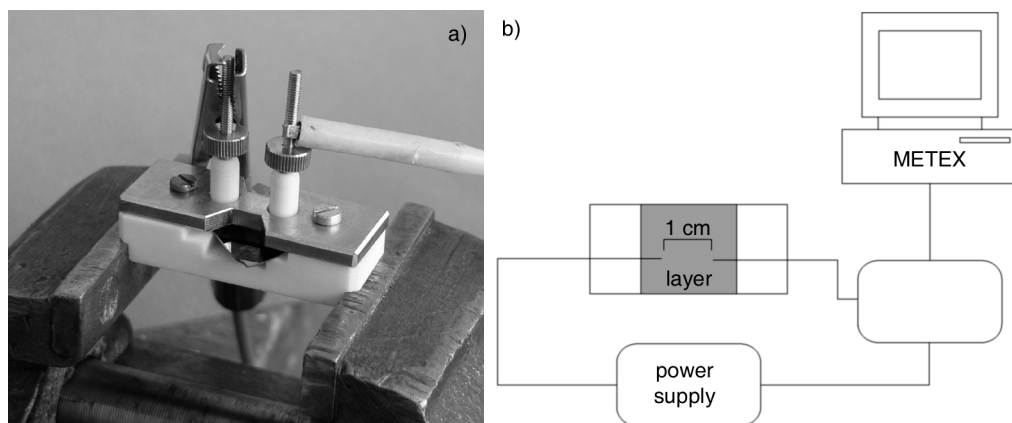


Fig. 1. Detailed view of the sample holder (a) and experimental set-up for measurements of resistivity (b)

The signal resulting from a liquid introduced onto the sample surface was measured as a function of time and recorded by the computerized system (Fig. 1b). The films contained from 20 wt. % to 39 wt. % of palladium which was connected with the Pd content in the substrate (maximum 44 wt. %).

The film structure was studied by electron diffraction and transmission electron microscopy (TEM). TEM investigations were performed with the JEOL-2000EX electron transmission microscope operating at 200 keV incident beam energy. The film topography was investigated with the atomic force microscope EXPLORER2000 in the non-contact mode in ambient atmosphere with the tip model MLCT-EXMT-A.

Absorption spectra were measured using the system which consisted of the DT-MINI-GS deuterium tungsten halogen light source, the S2000 miniature fiber optic spectrometer (Ocean Optics) which is a low-cost, high-performance system easily configured for UV-VIS-Shortwave NIR applications from 200 nm to 1100 nm.

3. Results and discussion

The TEM images of all the films show dark objects identified as Pd nanocrystals by the dark field image and EDSA techniques (Figs. 2, 3). In Figure 2a, diffused rings for Pd nanocrystals diffraction are seen, in Fig. 2b, diffraction for the C_{60} crystalline fcc type structure is shown and in Fig. 2c both types of diffraction patterns are presented.

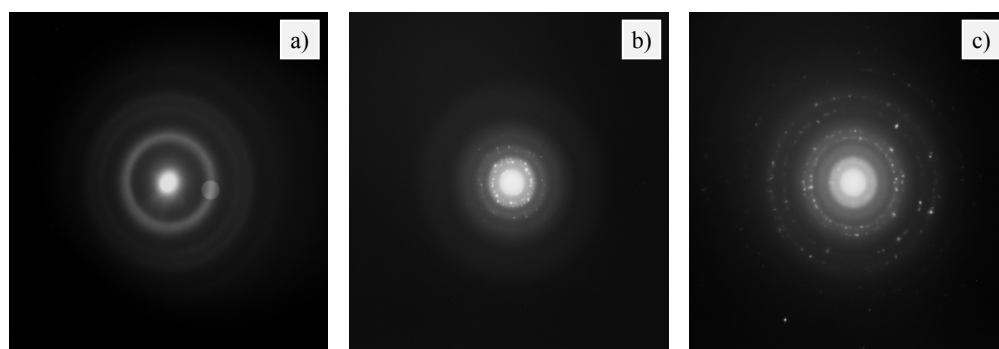


Fig. 2. EDSA patterns for the film containing 29 wt. % of Pd:
a) Pd(111), b) C_{60} (111), c) Pd(111) and C_{60} (111)

Pd nanocrystals are of fcc type and their sizes, determined from TEM images, range from 1.5 nm to 5 nm. The size distribution of Pd nanocrystal diameters film containing ~30 wt. % the Pd is presented in Fig. 3. It seems that with lowering the temperature of the source containing a palladium compound, the content of palladium in the film decreases, and the sizes of Pd nanocrystals increase.

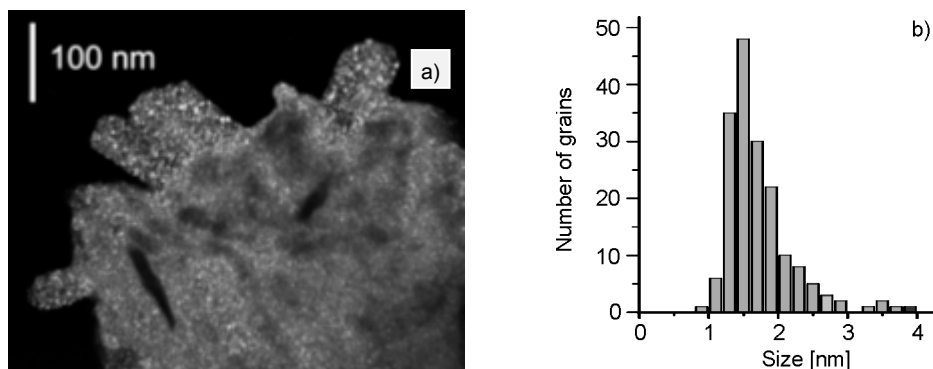


Fig. 3 TEM image (dark field mode) of a selected area (a) and size distribution for Pd nanocrystals observed in this area (b)

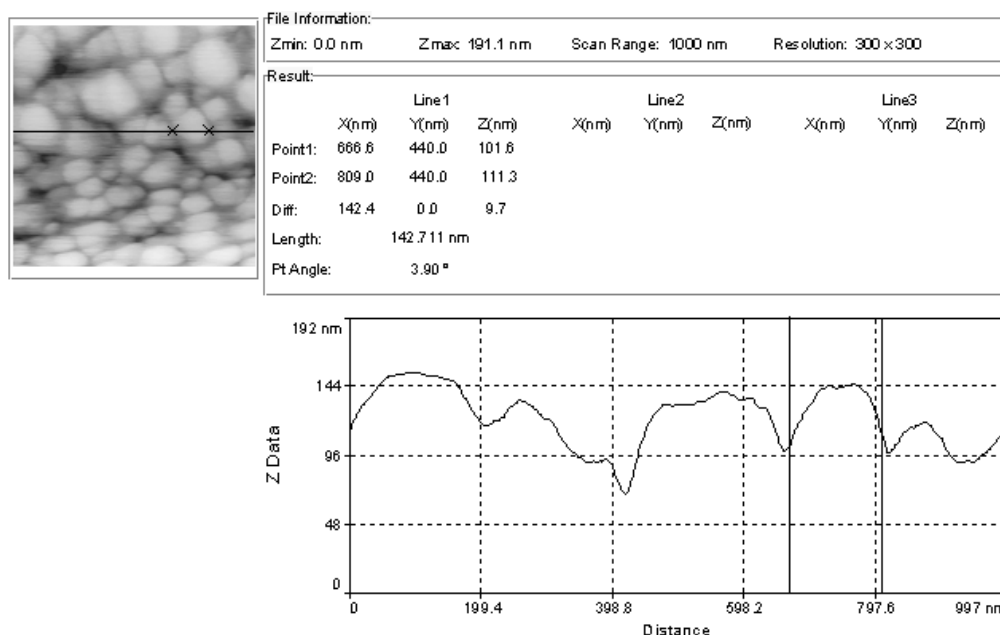


Fig. 4. AFM image of the film containing 23.5wt. % of Pd and the profile analysis along the line shown in the image

Analysis of the AFM images points to a developed surface of each sample. The samples with Pd content higher than 30 wt. % have dendrite-like topography (Fig. 5) while those with a lower Pd content have a hillock-like topography (Fig. 4). The profile analysis along a line enables one to determine nanocrystal sizes (diameter and height). The diameters of the objects forming the film surface with a lower Pd content are about 100–200 nm while those with a higher Pd range from 200 nm to 500 nm. The heights of the objects are the same in all cases.

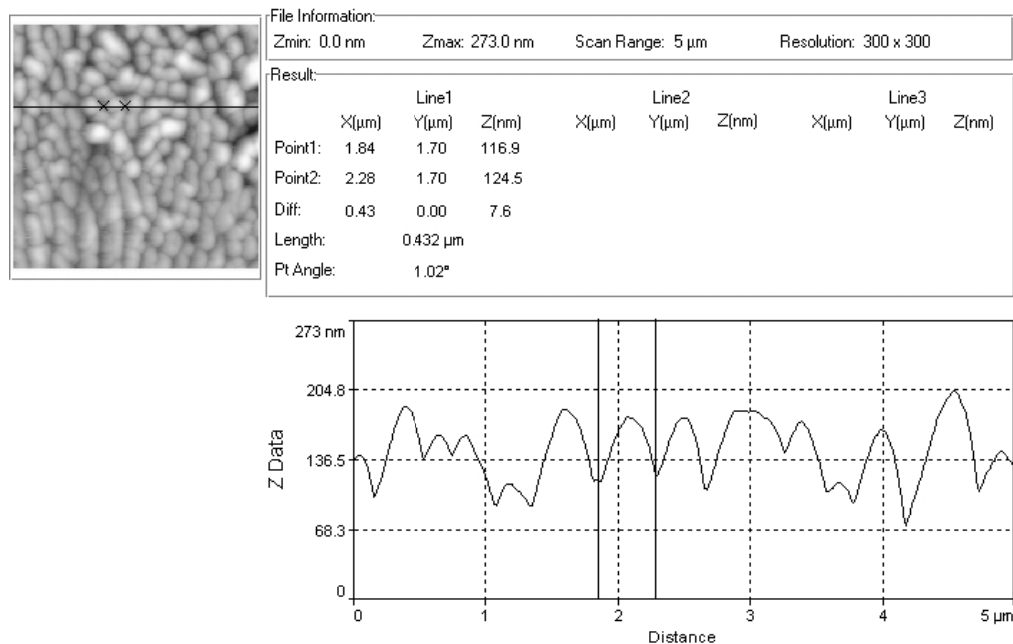


Fig. 5. AFM image of the film containing 30 wt. % of Pd and the profile analysis along the line shown in the image

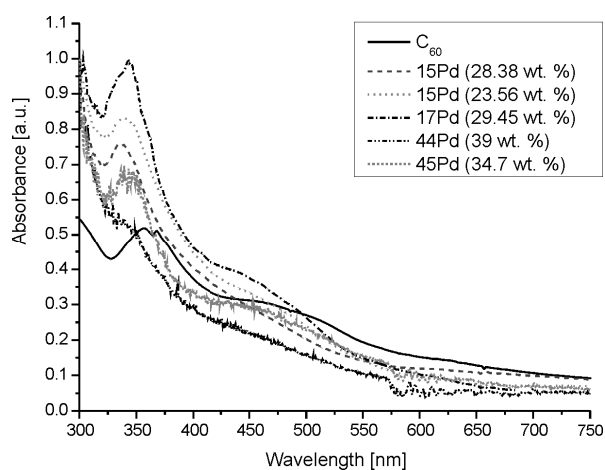


Fig. 6. Absorption spectra of Pd- C_{60} samples with various contents of Pd and of C_{60} film

UV-VIS absorption spectra of the samples with various Pd content and for a pure C_{60} film are presented in Fig. 6. In Table 1, the results of decomposition of these spectra into Gaussian shape bands are given (the adjustment coefficient was about 5%). In this table, the origin of particular bands is also presented according to Fig. 7. It can be seen that with increasing Pd content in the film, the maxima of the bands placed at ca. 290 and 340 nm shift toward higher wavelengths while the maximum of the band

at ca. 400 nm shifts towards lower wavelengths. The band located at the wavelength higher than 500 nm is much more sensitive to increase of Pd content. The origin of this band is not clear at the moment.

Table 1. Spectral parameters of the bands in the absorption spectra of samples with various Pd contents (λ – wavelength, $\Gamma_{1/2}$ – full width at a half maximum, I – intensity at a maximum)

Pd content	$h_g \rightarrow t_{1g}$			$h_u \rightarrow t_{1g}$			*		
	λ [nm]	$\Gamma_{1/2}$ [nm]	I [a.u.]	λ [nm]	$\Gamma_{1/2}$ [nm]	I [a.u.]	λ [nm]	$\Gamma_{1/2}$ [nm]	I [a.u.]
23.56 wt. %	331	77	121	427	116	62	501	142	20
28.38 wt. %	330	59	73	393	143	109	579	161	15
29.45 wt. %	337	50	74	402	171	148	599	45	10
34.7 wt. %	341	43	37	402	227	144			
Pure C ₆₀ film	341			467					

The resistivity was calculated based on measurements of voltage changes on the sample with known value of the current intensity. The results of resistivity measurements along a film for different liquids are presented in Table 2. The measurements of the film electric response in the presence of different liquids (ethanol, benzene) show a reversible time dependent current–voltage characteristics with short time (tenths of a second) of system response on the liquid dosage.

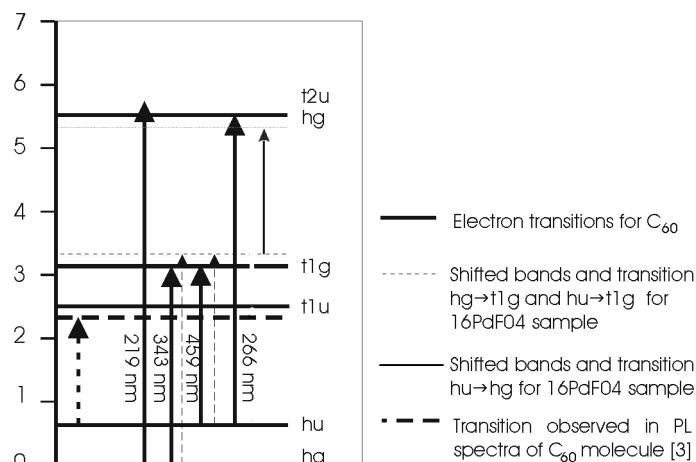


Fig. 7. Electronic structures of C₆₀ molecule and the system Pd + C₆₀ (for sample 16PdF04) [5]

Table 2. Resistivities along a film for different liquids

Pd content	Dry film [MΩ·cm]	Film wetted [kΩ·cm]	
		Ethanol	Benzene
27 wt. %	>>20	10 000	2500
34 wt. %			

4. Conclusions

The structure of the film formed from Pd nanocrystals placed in the Pd-C₆₀ matrix has been confirmed by the TEM results. In dark field images, Pd nanocrystals were visible with sizes between 1.5 nm and 5 nm (depending on the Pd content) and the related EDSA patterns showed the fcc type of their structure. For bigger areas, diffraction patterns connected with the C₆₀ fcc type crystalline structure have also been observed. On the other hand, the UV-VIS absorption spectra exhibit bands that may be attributed to the C₆₀-M (where M is a metal atom) electronic structure. Such spectra were also observed for the C₆₀-Hg system [5]. The band shifts observed in [5] were connected with changes in electronic structure of C₆₀ molecules due to the existence of a ligand field connected with metal atoms or particles.

AFM images show that the topography of the films also depends on the Pd content and is more complicated, and the surface is more developed for samples with a higher Pd content.

References

- [1] ALIVISATOS A.P., *Science*, 271 (1996), 933.
- [2] HAHN K.H., BEDULA K., *Scripta Metall.*, 23 (1989), 7.
- [3] HAUBOLD T., BOHN R., BIRRINGER R., GLEITER H., *Mater. Sci. Eng. A*, 153 (1992), 679.
- [4] MAIER R.R.J., BARTON J.S., JONES J.D.C., MCCULLOCA S., JONES B.J.S., BURNELL G., *Meas. Sci. Technol.*, 17 (2006), 1118.
- [5] GRYCUK T., CZERWOSZ E., *Fullerene Sci. Techn.*, 5/6 (1997), 1275.

Received 28 April 2007

Revised 16 February 2008